

Fig. 13 Cavity impedance seen from the beam: a) travelling-wave structure; b) standing-wave structure.

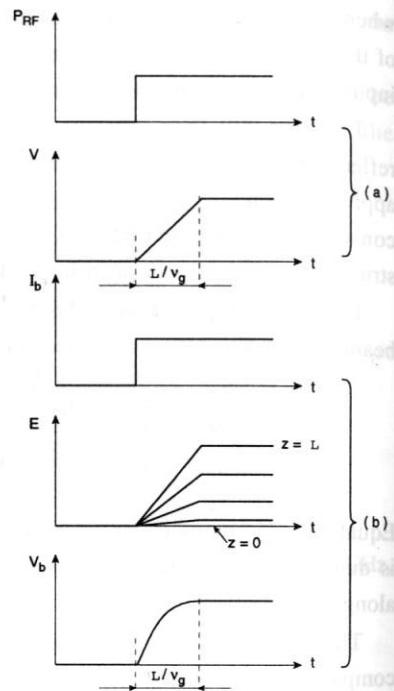


Fig. 14 Approximate transient responses of a travelling-wave cavity a) to RF-power step; b) to beam-current step.

References

1. R.E. Collin, "Field Theory of Guided Waves", IEEE, New York, 1991.
2. IIT Corporation, "Reference Data for Radio Engineers", Sams, Indianapolis, 1975.
3. J.N. Corlett, J. Johnson, G. Lambertson, F. Voelker, "Longitudinal and transverse feedback kickers for the ALS", Proc. Fourth European Particle Accelerator Conference, London, 1994, World Scientific, Singapore, 1994, pp. 1625-27.
4. P.M. Lapostolle, A. Septier (eds.), "Linear Accelerators", North Holland, Amsterdam, 1970.
5. G. Dôme, "The SPS acceleration system. Travelling wave drift tube structure for the CERN SPS", Proc. Proton Linac Conference, Chalk River, Canada, 1976, p. 138.

STANDING-WAVE STRUCTURES

E.V. KOZYREV

*Budker Institute of Nuclear Physics
630090 Novosibirsk, Russia*

The purpose of this lecture is to review the definitions of the main parameters that describe accelerating structures in general and standing-wave structures in particular. The lecture also contains some deductions from the classical standing-wave structure theory. Specific examples of structures developed at various accelerator centers illustrate the widespread feasibility of their application in accelerator physics.

1 Introduction

Basically all charged particles increase or decrease in kinetic energy when they travel in the direction of an electric field; a magnetic field may be used for deflection only. The acceleration can be along a straight path or along a closed orbit. For the first, linear accelerators are used, with single-pass acceleration; for the second, cyclic accelerators, with many-pass acceleration.

The simplest accelerators with constant electric field are used for low energy acceleration (a few tens MeV); these are Van de Graaff generators. In these, a high voltage is shared between a set of electrodes, creating an electric accelerating field between them, and the maximum energy of the particles is limited by the discharge effects of the high-voltage source.

Much higher energies may be reached by accumulative processes, but in this case the particle beam must be chopped into bunches. The beam will then arrive at accelerating electrodes in a sequence of bunches with gaps of comparable length between them. The gaps allow the polarity of the accelerating voltages to be switched periodically while the bunches are screened by a metallic pipe (drift tube) or similar device, so that the voltages applied to the beam particles will be multiplied by the number of beam passages. In principle any periodic electric fields could be used, but because of the technology derived from radio communications, sinusoidal radio-frequency fields are used. The layout of this accelerator type (known as Wideröe-type¹) is shown in Fig. 1.

The drift tube length L must satisfy the synchronism condition

$$L = \frac{\beta\lambda}{2}, \quad (1)$$

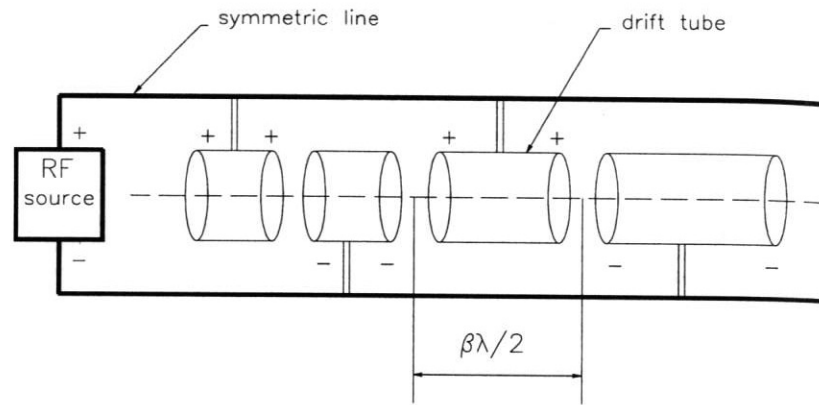


Figure 1: Wideröe-type accelerator.

where $\beta = v/c$, v is particle velocity, λ is free-space wavelength of the RF field, and c is the velocity of light.

Clearly the length of drift tubes for nonrelativistic particles will soon become prohibitive at higher energies unless the input RF frequency is increased. Higher-frequency generators became available only after World War II, as a consequence of radar developments.

At high frequency it is convenient to enclose the accelerating gap between drift tubes in a cavity and to make the resonant frequency of the cavity equal to that of the accelerating field. Figure 2 illustrates the simplest standing-wave accelerating structure.

The accelerator can consist of a series of such cavities fed individually with power sources. Also, several cavities can be coupled in single chain, forming a structure with many accelerating gaps fed by a common RF power source. As can be readily established, in this case for N cavities the full wall losses will be N times less than for one cavity if the energy gain is equal for the two cases, because the losses are proportional to the square of the accelerating electric field strength. The main advantages of coupled structures are:

- * the use of larger power supplies
- * a reduced number of power feeds
- * a reduced number of tuners, if the cells are coupled strongly
- * a possible saving of precious space in the beam line of the machine.

All such systems are characterized by a set of fundamental parameters, which may be introduced for a single right cylindrical cavity.

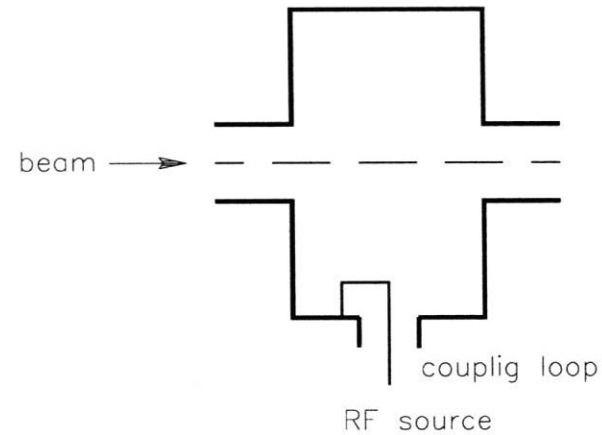


Figure 2: Standing-wave single-gap accelerating structure.

2 Basic Parameters of Accelerating Structures

2.1 Pill-box Cavity

Pill-box cavities are conventional for the accelerating structures in most cases (Fig. 3). For acceleration usually the TM_{010} mode is used. The field components of TM_{mnq} modes are given by

$$\begin{aligned}
 E_z &= \frac{\nu_{mn}^2}{a^2} J_m\left(\frac{\nu_{mn}}{a} r\right) \cos\left(\frac{\pi q z}{l}\right) \cos(m\varphi), \\
 E_r &= -\frac{a}{\nu_{mn}} J'_m\left(\frac{\nu_{mn}}{a} r\right) \sin\left(\frac{\pi q z}{l}\right) \cos(m\varphi), \\
 E_\varphi &= \frac{a^2}{\nu_{mn}^2} \frac{\pi q m}{l r} J_m\left(\frac{\nu_{mn}}{a} r\right) \sin\left(\frac{\pi q z}{l}\right) \sin(m\varphi), \\
 H_z &= 0, \\
 H_r &= -j \frac{a^2}{\nu_{mn}^2} \frac{m k}{Z_0 r} J_m\left(\frac{\nu_{mn}}{a} r\right) \sin\left(\frac{\pi q z}{l}\right) \sin(m\varphi), \\
 H_\varphi &= -j \frac{a}{\nu_{mn}} \frac{k}{Z_0} J'_m\left(\frac{\nu_{mn}}{a} r\right) \cos\left(\frac{\pi q z}{l}\right) \cos(m\varphi), \\
 k &= \frac{4\pi^2}{\lambda^2} = \sqrt{\left(\frac{\pi q}{l}\right)^2 + \left(\frac{\nu_{mn}}{a}\right)^2}.
 \end{aligned} \tag{2}$$

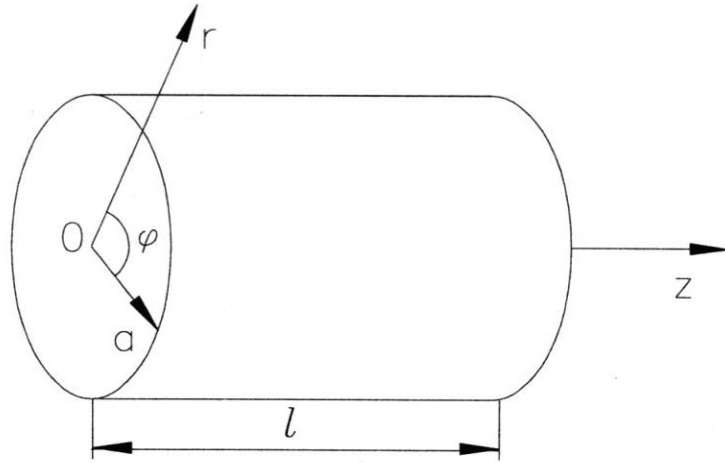


Figure 3: Cylindrical cavity.

Here ν_{mn} is the n th root of $J_m(x) = 0$ and λ is the free-space wavelength.

The TM_{010} mode has only two components:

$$\begin{aligned} E_z &= \frac{\nu_{mn}^2}{a^2} J_0\left(\frac{\nu_{mn}}{a} r\right), \\ H_\varphi &= -j \frac{1}{Z_0} J_1\left(\frac{\nu_{mn}}{a} r\right), \\ J'_0(x) &= -J_1(x). \end{aligned} \quad (3)$$

Thus we can see that for this mode the electric field does not depend on the longitudinal coordinate z . The resonant frequency is given by $\nu_{mn} = 2.4$:

$$\omega = c \frac{2.4}{a}, \quad \lambda = \frac{2\pi a}{2.4}. \quad (4)$$

2.2 Transit-Time Factor

Consider an accelerating gap and assume that the particle passes along the axis. In this case for a pill-box cavity the electric field of the TM_{010} mode is $E_z = E_0 \cos \omega t$.

If the particle passes through the center of the gap at $t = 0$ with a velocity v its coordinate is $z = vt$. We assume that the velocity of the particle does not change during the transit. Then the total energy gain is

$$\delta\varepsilon = qE_0 \int_{-l/2}^{+l/2} \cos\left(\frac{\omega z}{v}\right) dz = \frac{qE_0}{l} \frac{\sin(\theta/2)}{\theta/2} = qUT \quad (5)$$

where $\theta = \omega l/v$ is called transit angle, $U = E/l$ is the maximum voltage in the gap, and

$$T = \frac{\sin(\theta/2)}{\theta/2} \quad (6)$$

is the well-known transit-time factor. The transit-time factor shows the amount of energy gained when the particle travels in an electric field with a sinusoidal time variation compared with the case when the particle travels in a constant electric field. Usually the gap is chosen so that the value of T is about 0.8 to 0.9. In the more general case where the electric field is not homogeneous in the gap, the transit-time factor is given by

$$T = \text{Re} \left| \frac{\int E_z(z) \exp(j\omega t) dz}{\int E_z(z) dz} \right|. \quad (7)$$

2.3 Quality Factor

The most important characteristic of a cavity is its quality factor Q , which is defined as

$$Q = 2\pi \frac{\text{stored energy}}{\text{energy dissipated per cycle}} = 2\pi \frac{W_s}{T_o P_d} = \frac{\omega W_s}{P_d}, \quad (8)$$

where T_o is the period of oscillation, P_d is the average power loss in the cavity walls, and ω is the resonant frequency. If the cavity is coupled with external systems, the loaded quality factor Q_L is used with the same definition, but P_d is the power lost in the cavity and external systems.

The stored energy W_s in the resonant cavity is given by

$$W_s = \frac{\mu}{2} \int_V |H|^2 dv = \frac{\varepsilon}{2} \int_V |E|^2 dv. \quad (9)$$

Note that the magnetic field induces a surface current in the walls with a density $\vec{k} = \vec{H} \times \vec{n}$. Then for the power loss we obtain

$$P_d = \frac{1}{2} \int_S R_s |H|^2 ds, \quad (10)$$

where R_s is the surface resistance, $R_s = \sqrt{\mu\omega/2\sigma}$, where σ is the material conductivity and μ is the magnetic permeability. Then

$$Q = \omega \cdot \frac{\frac{\mu}{2} \int_V |H|^2 dv}{\frac{1}{2} \int_S R_s |H|^2 ds} = \frac{2}{\delta} \cdot \frac{\int_V |H|^2 dv}{\int_S |H|^2 ds}, \quad (11)$$

where $\delta = \sqrt{2/\mu\sigma\omega}$ is the skin depth.

It is also common to use the stored energy per unit length dW_s/dz . Then

$$Q = \omega \frac{dW_s/dz}{dP_d/dz}, \quad (12)$$

where dP_d/dz is the fraction of the power lost per unit length in the walls.

Considering the TM_{010} mode in a pill-box cavity one gets

$$Q = \frac{l}{\delta} \frac{a}{a+l}. \quad (13)$$

2.4 Shunt Impedance

An important quantity characterizing the efficiency of a cavity is its shunt impedance, as defined by

$$R = \frac{U^2}{2P_d}. \quad (14)$$

The shunt impedance R is a figure of merit which relates the accelerating voltage U to the power loss P_d in the cavity walls. The factor 2 in the denominator is applied to keep the analogy to Ohm's law $U_{eff}^2 = RP_d$, with $U_{eff} = U/\sqrt{2}$.

Very often the shunt impedance is defined as a quantity per unit length, and a more general definition is

$$R_L = \frac{E_z^2}{2P'_d} = \frac{R}{L}, \quad (15)$$

where L is the cavity length, E_z is the amplitude of the accelerating field and $P'_d = P_d/L$ is the power dissipated per unit length. Sometimes an incorrect shunt impedance Z is used where U is the integral of the field envelope along the gap. Then, to take care of the transit time factor T , the true shunt impedance becomes

$$R = ZT^2. \quad (16)$$

Also often used is the ratio of shunt impedance to quality factor,

$$\frac{R}{Q} = \frac{U^2}{\omega W_s}. \quad (17)$$

Since $W_s \sim U^2$ this expression depends only on the cavity geometry and allows comparison of the effectiveness of different cavities and structures. For a pill-box cavity one can get

$$\frac{R}{Q} = \frac{ZT^2}{Q} \cong 184.5 \cdot T^2 \left(\frac{b}{a}\right). \quad (18)$$

3 Examples of Standing-Wave Accelerating Structures

Single-gap pill-box cavities with TM_{010} mode of oscillation could be placed adjacent to each other (Fig. 4). The coupling between cavities is obtained in this case via drift tubes. Instead of capacitive coupling through the central passage, one can use "inductive" coupling slots. To reduce the capacitive coupling and increase the transit-time factor the small drift-tube nose is introduced. Thus a simple periodic cavity chain is formed.

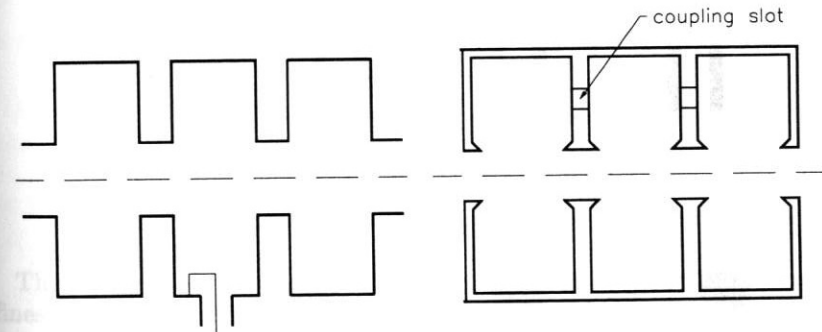


Figure 4: Simple cavity chain.

An analogy may be drawn between a chain of coupled cavities and chain of masses supported by springs. The excitation of this system may be described in terms of normal modes of oscillation. When we speak of cavity-chain modes, we refer to these normal modes, not to individual-cavity electromagnetic modes such as the TM_{010} mode. Each of these individual-cavity electromagnetic modes has its own set of normal modes of oscillation. For a chain of $N + 1$ cavities, there are $N + 1$ normal modes, one for each combination of phase shifts down the chain yielding $n\pi$ total phase shift, where $n = 0, 1, \dots, N$.

It is convenient to introduce here a mathematical model of the cavity chain used by Nagle². As a starting point it takes the lowest frequency mode of an isolated cavity, and treats a tank as a chain of one-dimensional harmonic oscillators coupled with strength k . Figure 5 shows schematically the model considered.

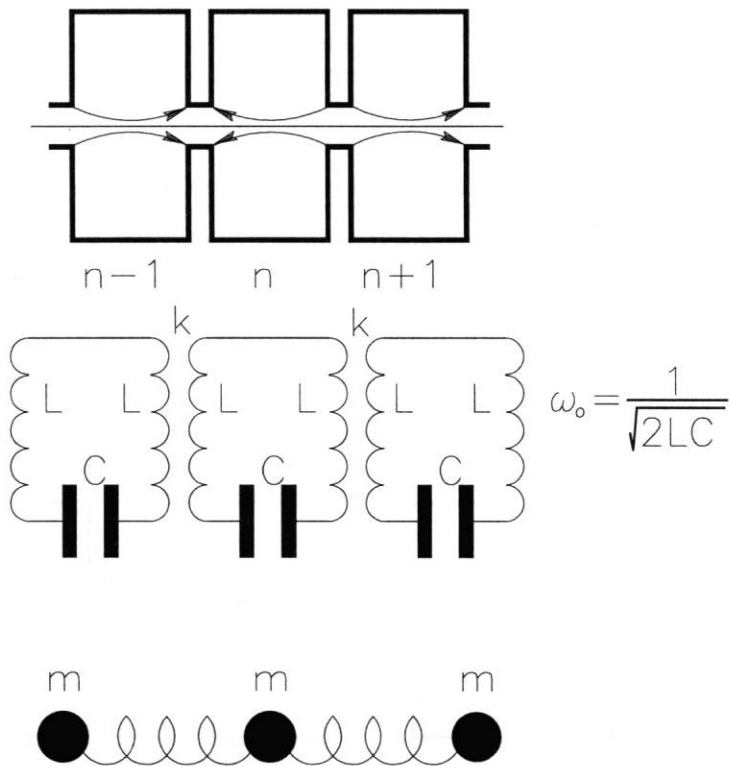


Figure 5: Coupled resonator model for a chain of coupled cavities, a chain of coupled lumped circuit constant resonators, or a chain of coupled masses.

The dispersion relation and amplitude of oscillation in cell n for a linear array (in the lossless case) are

$$X_n^{(q)} = \text{const} \cdot \cos\left(\frac{\pi q n}{N}\right) \exp(j\omega_q t), \quad n = 0, 1, \dots, N \quad (19)$$

$$\omega_q = \frac{\omega_0}{\sqrt{1 + k \cos(\pi q/N)}}, \quad q = 0, 1, \dots, N \quad (20)$$

where q is the number of the mode with resonant frequency ω_q , and ω_0 is the resonant frequency of the individual circuits. It is clear from Eq. (19) that in the lossless case the phase shift between fields in adjacent cavities is restricted to 0 or π for any mode. The dispersion curve for a simple chain of $N + 1$ coupled cavities, which also describes the behaviour of a series of coupled lumped circuits, is plotted in Fig. 6.

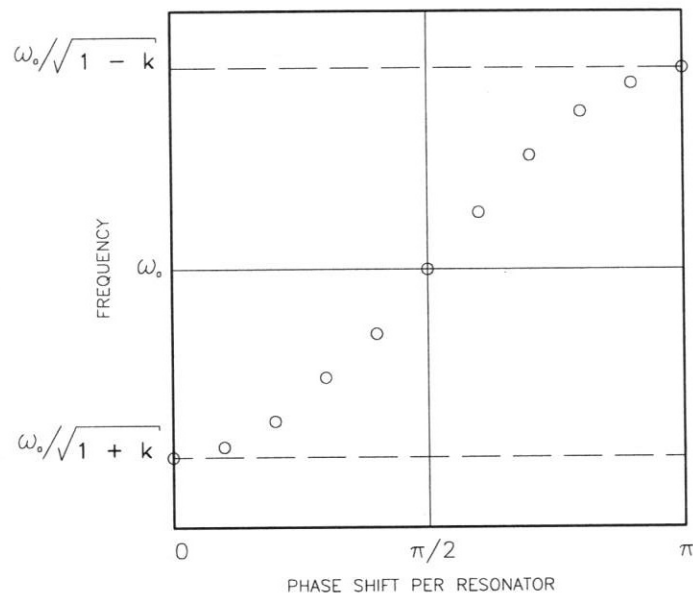


Figure 6: The dispersion curve for a simple chain of 10 coupled cavities.

The separation of the lower and upper cut-off frequencies (0 and π modes) defines the bandwidth $\Delta\omega$ of the structure. From Eq. (20) for $k \ll 1$ (small coupling) this is found to be

$$\Delta\omega \cong k \omega_0. \quad (21)$$

The separation of the zero and π modes from the ones nearest them is

$$\Delta\omega \cong k \omega_0 \frac{\pi^2}{4N^2} \quad (22)$$

whereas the separation of the $\pi/2$ mode from its nearest neighbors is

$$\Delta\omega \cong k \omega_0 \frac{\pi}{2N}. \quad (23)$$

Thus, for a given structure, the separation of modes near the $\pi/2$ mode is $2N/\pi$ times as great as the separation near zero and π modes. Operation at a particular mode without excitation of its neighboring modes requires that the Q of the structure be sufficiently high to prevent overlapping of the mode resonances. From Eqs. (22) and (23) it is clear that

$$Q_{0,\pi} > \frac{4N^2}{k\pi^2} \quad \text{and} \quad Q_{\pi/2} > \frac{2N}{k\pi}. \quad (24)$$

For example, if $Q = 10^4$ and $k = 10^{-2}$, the number of cavities in 0 or π mode structure cannot exceed ~ 16 without giving rise to concern about mode interaction. For the same Q and k , the $\pi/2$ mode structure can have ~ 157 cavities without overlapping of modes.

3.1 Zero-Mode Structures, Alvarez Structure

For zero mode (when $q = 0$) all cavities are excited in phase and have equal amplitudes of electromagnetic field. The distance between cavity centers, L , in this case must satisfy the synchronism condition

$$L = \beta\lambda. \quad (25)$$

The surface currents of the common walls between cavities are equal and flow in opposite directions. Therefore these walls may be removed.

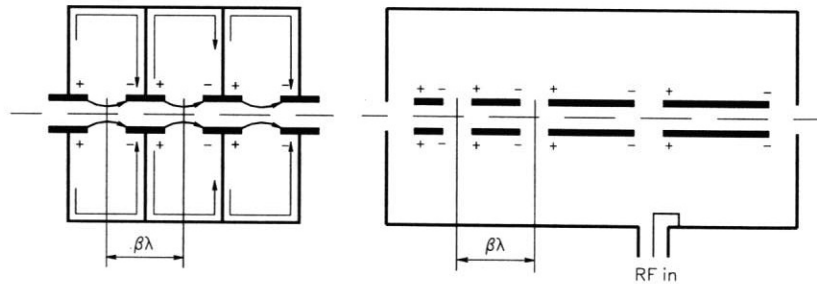


Figure 7: Coupled cavities with zero mode and Alvarez-type structure.

Since the TM_{010} mode is consequently independent of the longitudinal cavity size, the distance from one accelerating gap to the next is determined only by the particle velocities. A variant of zero-mode structure without the common walls between cavities is shown in Fig. 7. This scheme consists of placing the drift tubes in a single resonant tank such that the field has the same phase in all gaps. Such a resonant accelerating structure was invented by

Alvarez³ and was followed by the construction of a 32-MeV proton drift-tube linac powered by a 200-MHz source.

3.2 π -mode Structures

In the π -mode structures used for a wide range of synchrotrons and storage rings (where the particle velocities are constant), the phase shift from cavity to cavity is π radians in the lossless case (Fig. 8).

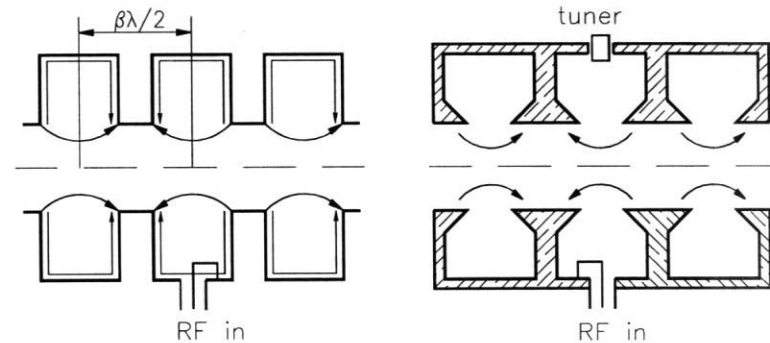


Figure 8: Coupled cavities with π -mode and nose-cone structure.

However, in the practical case with losses, energy must be supplied through excitation of adjacent modes to compensate the losses and this causes phase changes in the cavities. Thus, strictly speaking, operation in π mode is not possible. The phase deviation from π radians per cavity was given by Nagle², Knapp⁴, and Smith⁵ as

$$\Delta\varphi_{n,n-1} = \frac{2(1-k)^{1/2}}{Qk} \left(N - n + \frac{1}{2}\right). \quad (26)$$

Thus, the phase shift over the entire length of the structure is

$$\Delta\varphi_{0,\pi} = \frac{(1-k)^{1/2}}{Qk} N^2. \quad (27)$$

For example, if Q and k are the same as in the previous case and the number of cells is $N = 16$, the net phase shift is ≈ 2.5 radians, which is obviously excessive. To reduce the phase shift to a tolerable level, the coupling coefficient k of the structure would have to be increased; if this cannot be done, the number of cells must be decreased. Since it is technically impossible

to increase the coupling coefficient k to a value higher than a few percent, π -mode structures usually contain only a few cavities.

Figure 9 shows examples of five-cell structures operating with π mode (CERN, DESY).

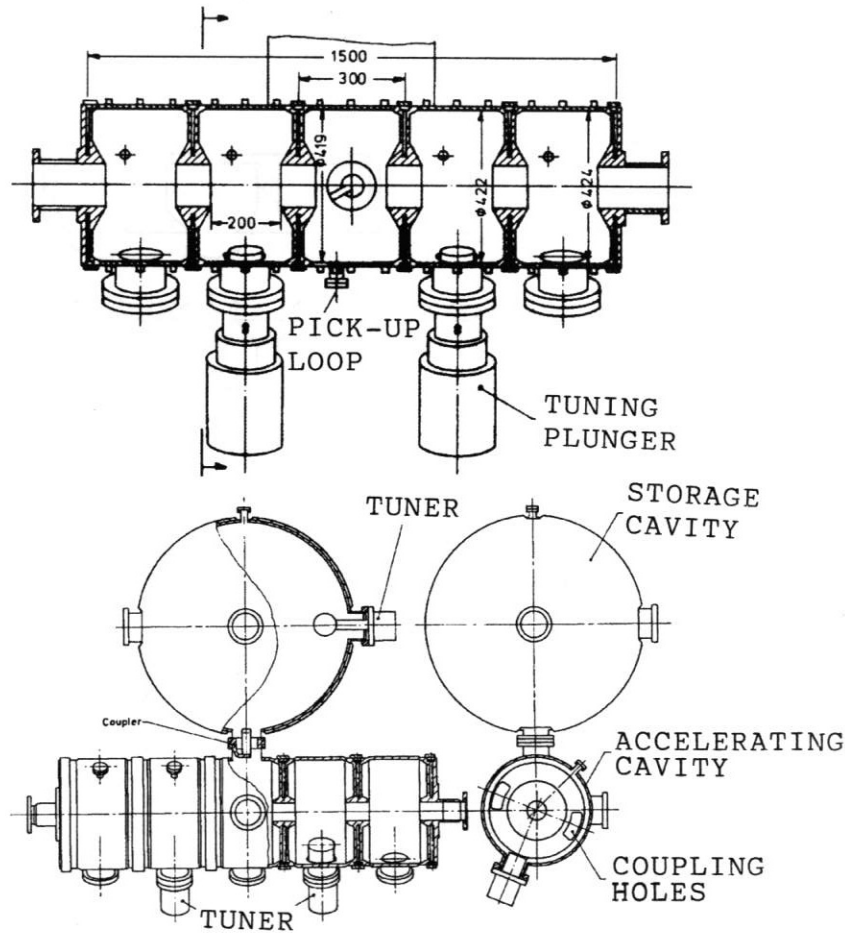


Figure 9: PETRA (DESY) and LEP (CERN) π -mode accelerating structures.

The low coupling coefficient, rather high quality factor, and proximity of neighboring modes cause the π -mode structure to be sensitive to beam-loading variations, and to heating and dimensional errors. To overcome these

disadvantages, various technical solutions are used; an example is the "parallel coupled" structure (Fig. 10).

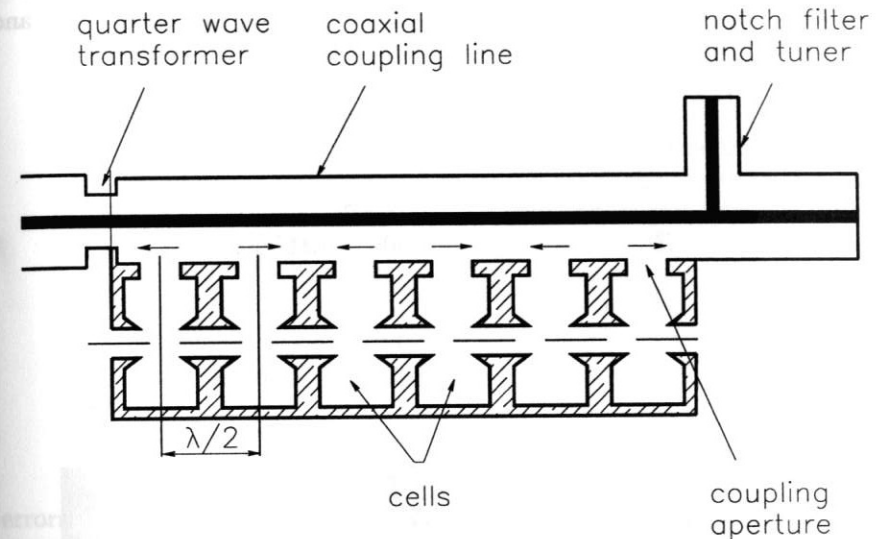


Figure 10: Side sectional view of "parallel coupled" structure.

In the coaxial coupling line the TEM standing wave becomes established. The coupling apertures with accelerating cavities are placed at points where the coaxial line wall current is maximum (the distance between them is $\lambda/2$). Thus all of the accelerating cavities are excited by the same current amplitudes with opposite phases.

The principal properties of this structure are as follows. The shunt impedance is maximized by using optimized cell shapes. Only one feed point is used for all cells. Overlap of the modes in the passband, a common problem when many cells are incorporated in one π -mode cavity, is eliminated because there is only one mode in the passband. A single mode occurs because the power does not propagate serially through the cells in the usual fashion. Other modes do occur in the coupling line, but their frequencies are sufficiently removed from the cell resonant frequency, that a negligible fraction of the energy appears in the cells. The notch filter closely approximates a short circuit at operating frequency. The tuning angle of the structure can be adjusted to compensate for variations in the beam loading by moving the tip of the center conductor of the notch filter parallel to the beam direction. This avoids the need for mechanical tuners in each cell.

Similar structures were made at Cornell University (USA, CESR) for use in an e^+e^- storage ring and at Budker Institute of Nuclear Physics (BINP Russia) for a racetrack microtron. Figures 11 and 12 show the 9-cell BINP "parallel coupled" cavity structure and the interior of the coaxial line and accelerating cavity. The parameters of this structure are listed below:

operating frequency	915	MHz
number of cells	9	
total structure length	1.5	m
quality factor of coaxial line	5000	
quality factor of accelerating cavity	18000	
shunt impedance (R)	30	$M\Omega/m$
R/Q of accelerating cavity	213	Ω
R/Q of coaxial line	20	Ω
coupling coefficient k	0.84	%
accelerating gradient	4	MV/m

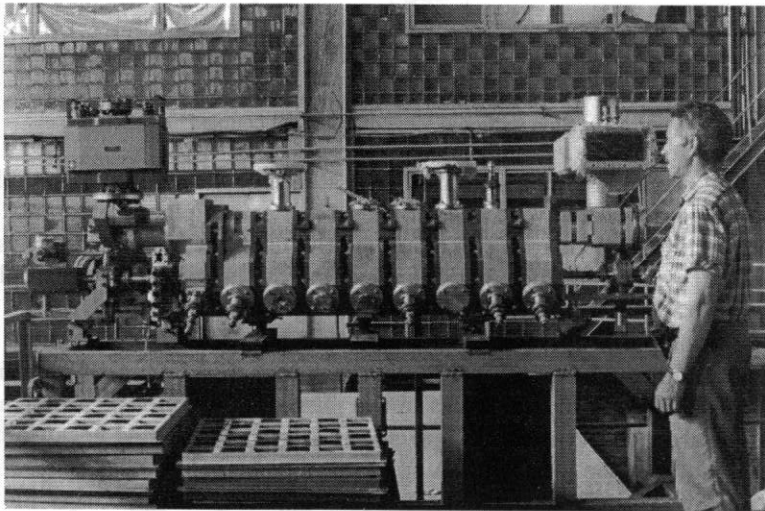


Figure 11: General view of BINP "parallel coupled" structure.

3.3 $\pi/2$ -mode Structures

The advantages of these structures were shown by Knapp⁴ and Giordano⁶. The $\pi/2$ mode is much less sensitive to beam loading variations and to dimensional

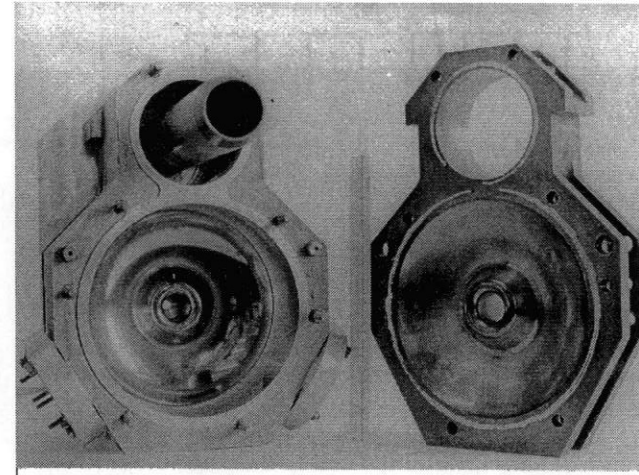


Figure 12: Inner structure of the coaxial line and accelerating cavity.

errors. For the $\pi/2$ mode even cavities have the same amplitudes, odd cavities are empty, and there is a π -radian phase shift between adjacent even cavities. This is shown in Fig. 13(a). This geometry would be suitable for accelerator applications if the synchronous condition were satisfied:

$$L = \frac{\beta\lambda}{2}, \quad (28)$$

where β is particle synchronous velocity in units of light velocity.

If this geometry were used directly, the efficiency of the system for particle acceleration would be extremely poor, because half of the accelerator provides no energy transfer to the beam. However, the model developed here has no restriction on the geometrical shape of the adjacent cavities. In fact, the chain may look biperiodic (alternating-periodic structure – APS), as shown in Fig. 13(b), and if the cavities are all tuned to the same uncoupled resonant frequency, the $\pi/2$ -mode characteristics will remain identical to that for the periodic system. This observation allows consideration of a multitude of possible cavity configurations, all with the same mode characteristics. One possible configuration, which has a high shunt impedance (up to 40 $M\Omega/m$), is the "side-coupled" structure (SCS), shown in Fig. 13(c).

This scheme has substantial advantages over many of the others considered, namely:

- Maximum length along the beam line is available for accelerating field,

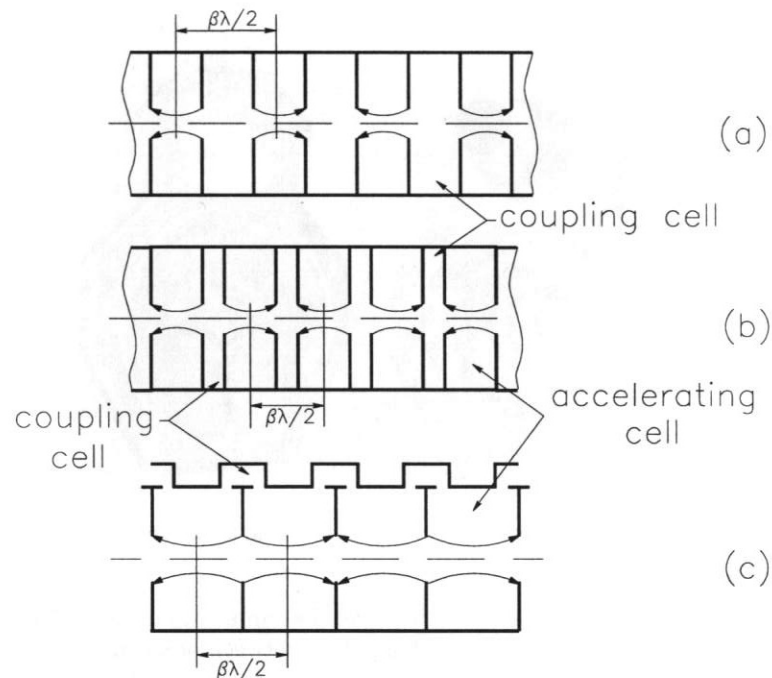


Figure 13: $\pi/2$ -mode operation of a cavity chain: (a) periodic cavity chain; (b) biperiodic cavity chain; (c) side-coupled chain.

which leads to optimum shunt impedance.

b) Only small slots at the outer wall are required for coupling, allowing almost complete freedom to design the on-line cavity for maximum shunt impedance. For example, introducing capacitive loading near the beam line by putting "nose cones" in the cavities increases the transit time factor T and also the average axial electric field for a given stored energy. Curving the outer walls also gives minimum power loss for a given stored energy.

c) The offset cavity stores very little energy even in a typically lossy case and thus little attention need be paid to its Q factor or geometry.

An example of a biperiodic structure is shown in Fig. 14. This structure was developed at BINP (Russia) and used in an electron linear accelerator, the

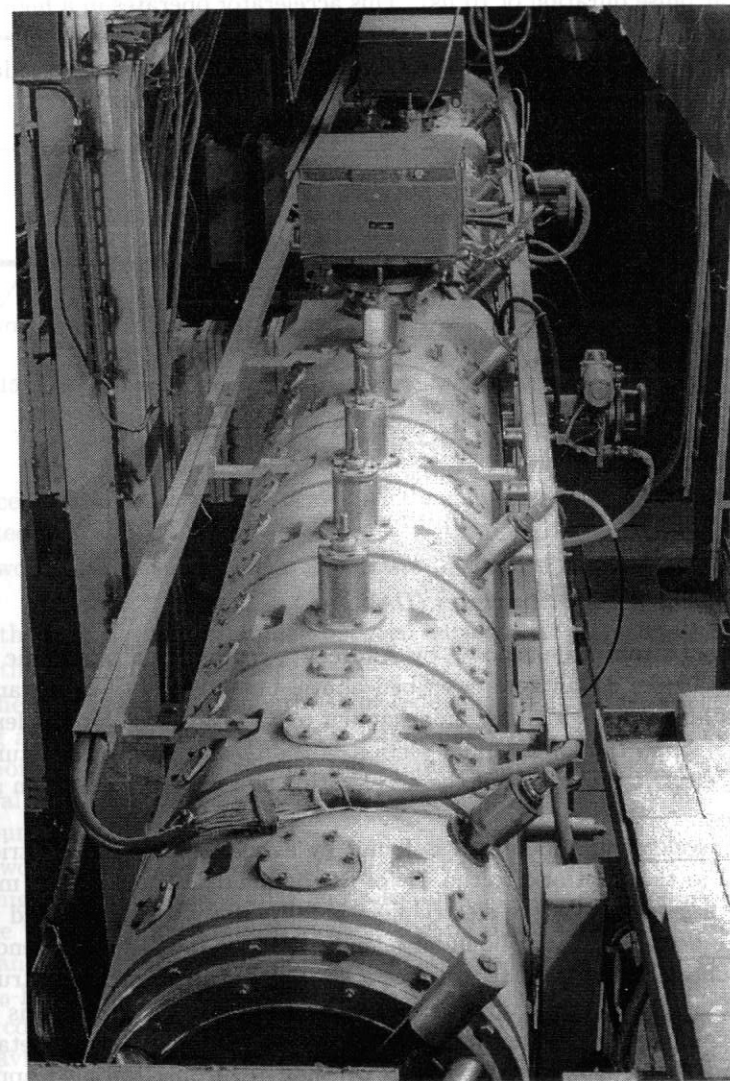


Figure 14: BINP biperiodic structure for injector of VEPP-4.

injector of the VEPP-4 storage ring. The accelerator consists of two identical sections fed by the high power pulse RF generator gyrocon (output power of 65 MW at pulse duration of 10 μ s). This accelerator operates in a high stored energy mode and its filling time is rather short compared with the power source pulse length. Therefore the value of the structure shunt impedance is not critical. The main accelerator parameters are listed below:

operating frequency	430	MHz
mode	$\pi/2$	
number of structures	2	
number of structure cells	19 (10+9)	
quality factor of structure	20000	
quality factor of accelerating cavity	22000	
shunt impedance (R)	12	M Ω /m
R/Q of accelerating cavity	200	Ω
coupling coefficient k	10.6	%
accelerating gradient	8	MV/m
full energy gain	55	MeV
electron beam pulse current	33	A

3.4 Disk and Washer Structures (DAW)

This type of structure, proposed by Andreev⁷, represents a biperiodic structure with all the advantages described above, but, instead of a fundamental TM_{010} pill-box mode, a higher mode similar to TM_{020} is used for acceleration. Figure 15 shows the longitudinal section of a disk and washer structure and gives the electric field maps of the accelerating and coupling modes in such a structure.

The accelerating mode field is found by assuming that the electric field is normal to the right and to the left of the boundary. The coupling mode is found by assuming that the electric field is tangential to the right and to the left of the boundary. Both boundary conditions give the same frequency and we can consider the DAW structure as a variation of the biperiodic structure.

For the accelerating mode there is a distance from the cavity axis where the longitudinal field E_z vanishes and where it is possible to insert metallic or dielectric rods to support the washers without disturbing the field appreciably. The full-circumference slot between the washers and the outer cylinder produces a strong coupling between cells of about 40%. The theoretical shunt impedance in this case is higher because of the lower current density on the tank walls. However, in actual operation in many cases the supporting rods

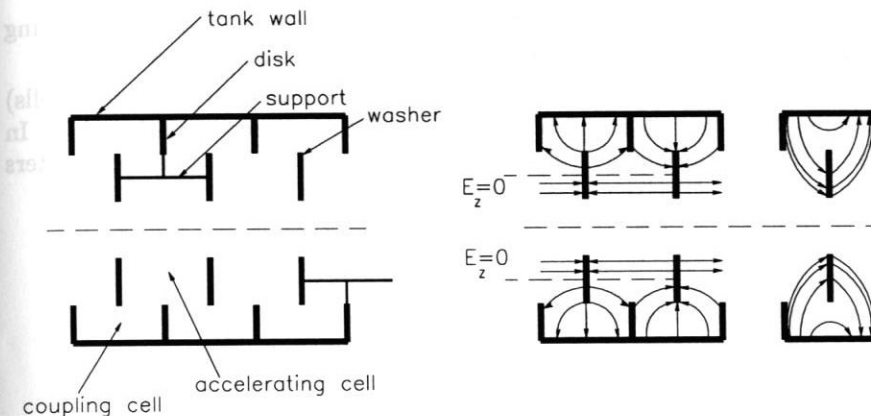


Figure 15: Disk and washer structure and electric field of the accelerating mode (left) and that of the coupling mode (right).

produce such high losses that nearly all the gain in shunt impedance is compensated.

Two of the most attractive properties of the disk and washer structures are:

- * the high degree of coupling between adjacent RF cavities,
- * the high shunt impedance.

The first property is important for reducing the structure's sensitivity to tuning and assembly errors, beam loading effects, and transients. The second is important for possible savings from reduced RF power and reduced heat removal or higher average accelerating gradients for the same investment in RF sources.

Two aspects of the DAW geometry identified as needing more investigation were higher-order-mode studies and selection of a suitable support technique for the washers that dissipate most of the RF heat. Because the operating passband encompasses the frequency region from the TM_{010} -like mode to the TM_{020} -like mode (a consequence of the DAW's main asset - its high coupling coefficient), it was obvious from published mode charts for right pill-box cavities that the TE_{111} -like, TM_{110} -like, TE_{211} -like and TM_{210} -like mode passbands would be in the vicinity of the $\pi/2$ operating mode over the practical range of the geometric dimensions. Therefore, for any structure, it is important to know the mode locations and their field distributions, mode RF characteristics as a function of geometric changes, and mode influence on beam transmission. With this information, geometries can be selected and methods

can be employed to minimize or eliminate unwanted effects. Calculations using newly developed computer codes make it possible to solve this problem.

Figure 16 shows two types of DAW structure (with twelve and nine cells) that have been installed and tested in the TRISTAN accumulating ring. In these structures the single radial stem support was used. The main parameters calculated for the twelve-cell structure are shown below:

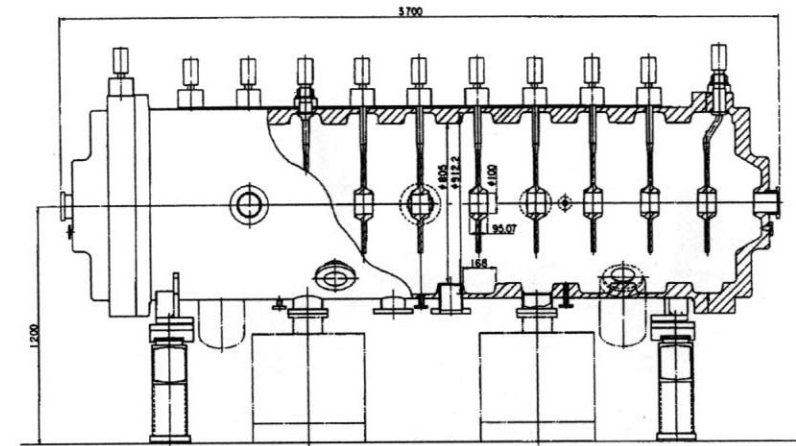
operating frequency	500 MHz
transit time factor	0.765
shunt impedance (effective)	44.76 M Ω /m
Q (for copper cavities)	112500
R/Q	680 Ω /m
length	3.7 m
coupling coefficient	0.4

The achieved shunt impedance was approximately 0.6 of the calculated one, apparently because of non-optimal length of the radial stem. This length must be close to $\lambda/4$ (quarter of free-space wave length). In this case the current distribution along the stem will be such that at the point where the stem is connected to the washer the current will be zero. The frequency of the operating mode also will be the same as without stems.

An example of such a solution is the DAW standing-wave structure linac-reinjector for the SIBERIA-2 SR complex (Russia) (Fig. 17). Each washer is supported by three radial stems, and the length of each is close to $\lambda/4$. The stems are dispersed homogeneously along the circle.

As a result of numerical and experimental studies the optimal geometry of the DAW structure provided a very high shunt impedance of 95 M Ω /m and the absence of high-order modes near the operating TM_{02} mode. The nearest non-operating TM_{11} mode has the 20 MHz higher frequency. The dispersion curves of this structure are shown in Fig. 18 and its main characteristics are presented below:

operating frequency	2797 MHz
shunt impedance (effective)	95 M Ω /m
Q (for copper cavities)	28000
R/Q	3.4 k Ω /m
length	6 m
coupling coefficient	0.4



S. Inagaki / Disk-and-washer cavities

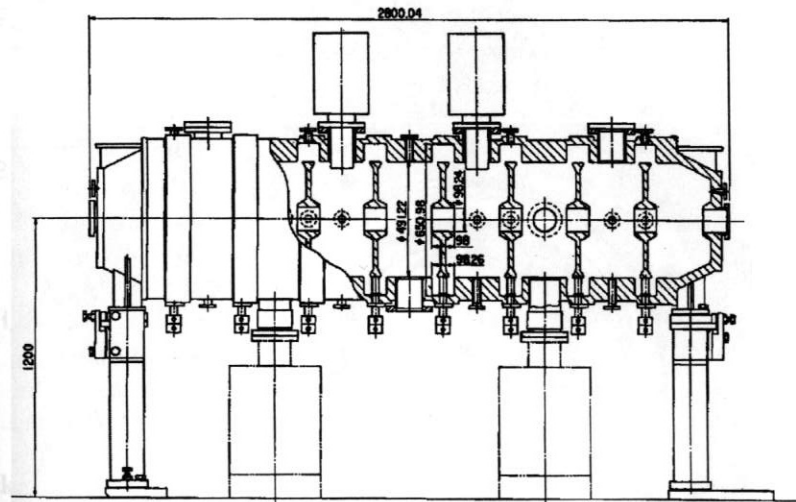


Figure 16: Two types of TRISTAN DAW structures.

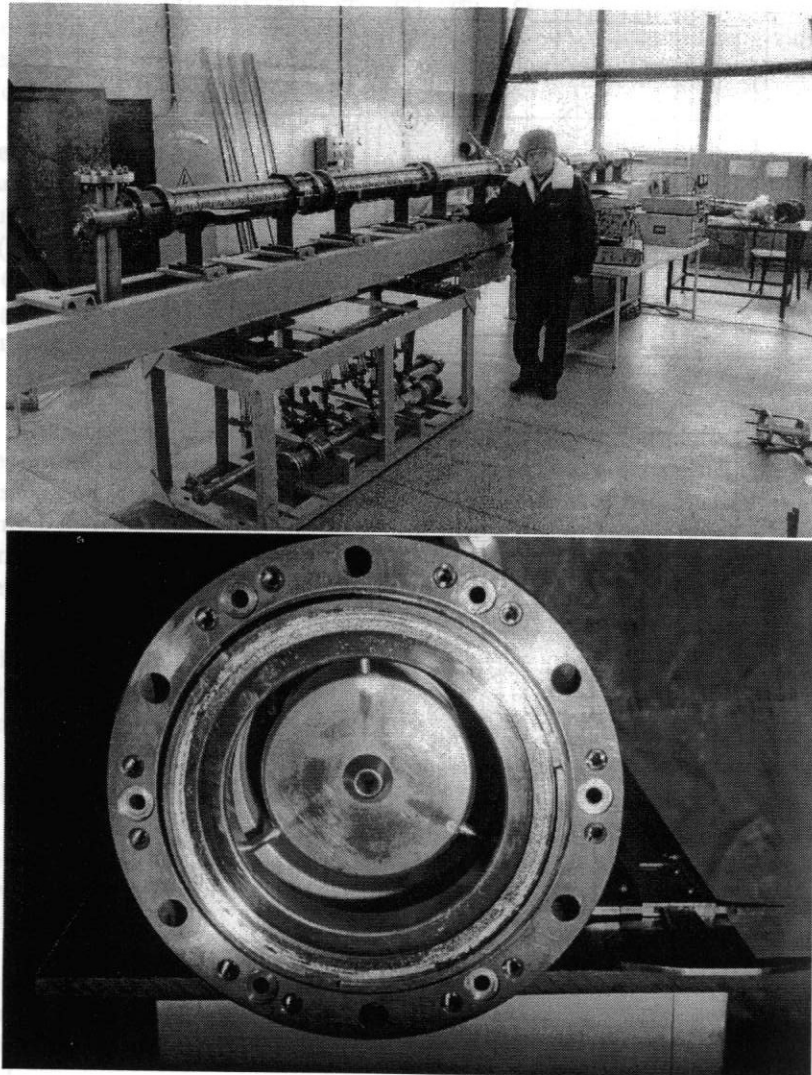


Figure 17: Layout of SIBERIA-2 linac-preinjector and interior of its DAW structure.

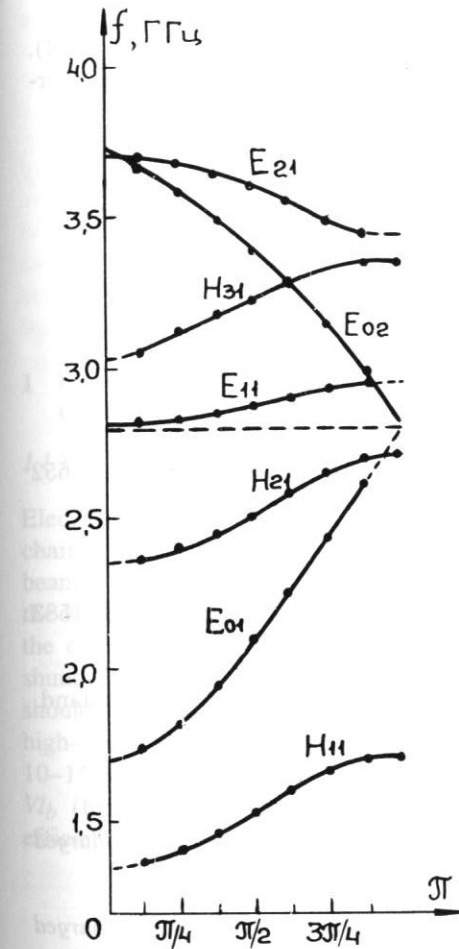


Figure 18: Dispersion curves of SIBERIA-2 DAW structure.

Acknowledgments

The author would like to thank prof. M.M. Karliner for discussions and valuable suggestions.

References

1. R. Wideröe, *Archiv für Elektrotechnik*, 21, 387 (1928).
2. D.E. Nagle, in *Proc. 1964 Linear Accel. Conf.*, MURA 714, pp. 21-30 (1964).

3. L.W. Alvarez, *Phys. Rev.*, **70**, 799 (1946).
4. E.A. Knapp, in *Proc. Linear Accel. Conf.*, MURA 714, pp. 31–59 (1964).
5. T.I. Smith, Standing Wave Modes in a Superconducting Linear Accelerator, HEPL 437, Stanford (1966).
6. S. Giordano, *IEEE Trans. Nucl. Sci. NS-12* **3**, pp. 213–216 (1965).
7. V.G. Andreev, *Sov. Phys. Techn. Phys.* **13**, 1070 (1969).

Bibliography

- P.H. Sloan and E.O. Lawrence, *Phys. Rev.* **38**, 2021 (1931).
- E.A. Knapp *et al.*, *Rev. Sci. Instr.* **39**, 979 (1968).
- J.C. Slater, *Rev. Mod. Phys.* **70**, 799 (1946).
- T. Nishikawa, S. Giordano, and D. Garter, *Rev. Sci. Instr.* **37**, 652 (1966).
- E.A. Knapp, *IEEE Trans. Nucl. Sci.* **3**, 118 (1965).
- D.E. Nagle, E.A. Knapp, and B.C. Knapp, *Rev. Sci. Instr.* **38**, 1583 (1967).
- P. Lapostolle and A. Septier, Eds, *Linear Accelerators* (North Holland, Amsterdam, 1970).
- R.M. Sundelin *et al.*, *IEEE Trans. Nucl. Sci.* **24**, 1686 (1977).
- G.I. Budker *et al.*, in *Proc. 5th All-Union Workshop on Accel. of Charged Part.*, Dubna, v. 1, 280 (1977).
- V. Akimov *et al.*, in *Proc. 11th All-Union Workshop on Accel. of Charged Part.*, Dubna, v. 1, 268 (1989).
- A. Gamp, in *CAS - RF Eng. for Part. Acc. Proc.*, 3–10 April 1991, CERN 92-03, vol. II, 396 (Geneva, 1992).
- S.O. Schriber, *IEEE Trans. Nucl. Sci.* **30**, 3542 (1983).
- V. Korchuganov *et al.*, in *Proc. EPAC 94*, London, v. 1, 739 (1994).
- S. Inagaki, *Nucl. Instr. Meth. A* **251**, 417 (1986).

SUPERCONDUCTING CAVITIES

W. WEINGARTEN
CERN, Geneva, Switzerland

The basic properties of superconducting cavities for electron accelerators are discussed with special emphasis on the following topics: technical motivation for the use of superconducting cavities; surface impedance; the critical field of superconductors; anomalous losses; materials other than niobium; technological achievements for accelerating cavities.

1 Introduction: Technical Motivation for the Use of Superconducting Cavities

1.1 The Mains-to-Beam-Power Conversion Efficiency

Electrical power from the mains to the beam is transferred via the following chain: high-voltage power supply — klystron — waveguide — RF cavity — beam. For copper cavities the largest power loss has to be tolerated between the RF cavity and the beam. In order to establish the accelerating voltage V in the cavity, RF currents are induced at its surface, generating the heat P_c . A shunt impedance $R = V^2/(2P_c)$ is defined¹ to account for these RF losses. R should be as large as possible. RF accelerating cavities manufactured from high-conductivity copper have shunt impedances (per unit length) of typically 10–15 M Ω /m. With the beam current I_b (d.c. component), the beam power $P_b = VI_b$ (for the particle riding on the crest of the RF wave), the conversion efficiency is defined as

$$\eta = \frac{P_b}{P_b + P_c} = \frac{1}{1 + \frac{P_c}{P_b}} = \frac{1}{1 + \frac{V}{2RI_b}} \quad (1)$$

For the LEP RF cavity (copper) with $R = 43$ M Ω , $I_b = 6$ mA, $V = 3$ MV we get $\eta \approx 15\%$.

As can be inferred from Eq. (1), normal-conducting (nc) cavities made from copper offer high conversion efficiencies for high beam currents and low accelerating voltages. The shunt impedance R of an RF cavity is related to its Q value by $R = (R/Q) Q$. (R/Q) is independent of the RF frequency and is determined by the geometry of the cavity. The Q value for its part is inversely proportional to the surface resistance R_s , $Q = G R_s^{-1}$, with G another geometrical constant (of typically 250 Ω). Hence, in order to have large shunt impedances,